Exploring the utility of Sentinel-2 MSI derived spectral indices in mapping burned areas in different land-cover types

Article *in* Scientific African · September 2020

DOI: 10.1016/j.sciaf.2020.e00565

CITATIONS
5

READS
155

3 authors:

Kudzai Mpakairi
University of the Western Cape
21 PUBLICATIONS **97** CITATIONS
SEE PROFILE

Henry Ndaimani
University of Zimbabwe
36 PUBLICATIONS **264** CITATIONS
SEE PROFILE

Blessing Kavhu
Zimbabwe Parks and Wildlife Management Authority
18 PUBLICATIONS **72** CITATIONS
SEE PROFILE

Scientific African 10 (2020) e00565

Contents lists available at ScienceDirect

Scientific African

journal homepage: www.elsevier.com/locate/sciaf

Exploring the utility of Sentinel-2 MSI derived spectral indices in mapping burned areas in different land-cover types

Kudzai Shaun Mpakairi[a,*], Henry Ndaimani[a], Blessing Kavhu[b,c,d]

[a] University of Zimbabwe, Department of Geography and Environmental Science, Box MP 167, Mount Pleasant, Harare, Zimbabwe
[b] Zimbabwe Parks and Wildlife Management Authority Headquarters, P O Box CY140 Causeway, Borrowdale, Harare, Zimbabwe
[c] Department of Geography and Environmental Studies, Stellenbosch University, Private Bag X1, Matieland 7602, South Africa
[d] Centre for Complex Systems in Transition, Stellenbosch University, Stellenbosch 7600, South Africa

ARTICLE INFO

Article history:
Received 22 May 2020
Revised 31 August 2020
Accepted 16 September 2020

Keywords:
Random forest
BAI
GEMI
Classification

ABSTRACT

The difference in structure and composition of landcover types requires accurate mapping of burned areas for post-fire ecological assessments. Spectral indices for burned area mapping are mostly hard-coded to particular environments. However, the best post-fire spectral index to use for burned area mapping in most unstudied landcover types is not known. In this study, out of nine burned mapping indices optimised using the red-edge band, we tested which index outperformed the others in different land cover types. We used the Random Forest (RF) classifier to detect burned areas from Sentinel 2A imagery in four study sites and assessed the classification accuracy. We found out that, the Burned Area Index (BAI) and Global Environmental Monitoring Index (GEMI) spectral indices outperformed other indices in open shrublands, evergreen forest and in needle-leaved and semi-deciduous forests. The lowest performing spectral indices in the four study sites were Optimised Soil Adjusted Vegetation Index (OSAVI), Normalise Burn Ratio (NBR), and Normalise Difference Vegetation Index (NDVI). We recommend that for future studies, researchers and ecologists should use BAI and GEMI in mapping fires in open shrublands, evergreen, needle-leaved and semi-deciduous forests. Our results provide necessary insight for burned mapping algorithms and the accurate estimation of post-fire carbon emission with uni-temporal spectral indices in open shrublands, evergreen, needle-leaved and semi-deciduous forests.

Introduction

Overwhelming evidence has been published that suggests wildfires are inherently crucial in the distribution of species and the maintenance of structure and function of most ecosystems (e.g. savannahs). However, wildfires have done more harm than good in most environments they frequently burn. For instance, the 2018 Camp fire in California lasted over three weeks and destroyed 10 000 homes [38]. Worldwide 340 million hectares of land burn annually (the combined size of India

* Corresponding author.
E-mail address: kudzishaun@gmail.com (K.S. Mpakairi).

https://doi.org/10.1016/j.sciaf.2020.e00565

and Jersey) and the most burned ecosystems are savannahs, open shrublands and subtropical grasslands [22]. Although wildfire incidences have been decreasing globally, there has been an increase in burned areas in most environments [46]. However, several authors argue that the reduction stems from the inaccurate estimates of burned areas [13].

Some of the steps followed in wildfire management include identifying areas that are likely to burn [36] and being able to map burned areas [27]. The method used for delineating and mapping burned areas has a bearing on the accuracy of the burned area. The advent of remote sensing and freely available imagery has allowed ease and high accuracy in burned area mapping through the use of spectral indices. Spectral indices have been widely used with active and passive sensors at varying resolutions. The extent of the area burned often determines the ideal spatial resolution to use for mapping a burned area [24]. However, owing to the unavailability of high spatial resolution imagery, most studies on burned area mapping have used low and medium spatial resolution sensors for the estimation of burned areas (e.g. Advanced Very High-Resolution Radiometer (AVHRR) and Moderate Resolution Imaging Spectroradiometer (MODIS)). The problem with using low spatial resolution sensors is their inability to detect pixels with spectral mixing. For instance, MODIS was observed to underestimate fires in Alaska by 15-70% [32]. Uncertainty in wildfire mapping has a huge bearing on detection algorithms, hence the need for sensors that can provide high accuracy estimates, like the freely available Sentinel-2. Sentinel-2 is a medium resolution sensor that was launched in 2016 for land and water monitoring by the European Union (EU) Copernicus Programme. Sentinel-2 has not been explored fully for wildfire mapping although the sensor has a better spatial resolution (10-60m resolution with 13 bands) than most medium resolution sensors. More importantly, Sentinel-2 also provides imagery in the red-edge band [9]. The red-edge band, particularly the one closer to the red band in Sentinel-2, is important in vegetation monitoring since it is sensitive to chlorophyll changes [9,12]. The sensitivity of the red-edge band is relevant especially when trying to detect burned areas with vegetation spectral indices. Besides, most spectral vegetation indices that use the red-edge band perform better than those that do not use it. For instance, Filipponi [20] found out that the Burned Area Index for Sentinel-2 (BAI2) had higher spectral discrimination of burned areas than other spectral indices.

Burned areas respond more in the red, near-infrared and shortwave infrared spectral regions and most spectral indices for burned mapping utilise these bands. Previous studies have proposed several spectral indices for burned area mapping however these indices are mostly hard-coded to particular environments. For example, BAI performs well in Mediterranean environments [8] and Char Soil Index (CSI) discriminates burned areas well after high burn severity [50]. However, the response of burned areas in these regions varies with burn severity, landcover type and other ancillary factors. Also, using a particular spectral index for burned mapping outside the environment it was designed for can lead to high uncertainty [49]. Given this variability, there is a dearth in literature on spectral indices to use when mapping burned areas in different environments in different environ. The most accurate spectral index for mapping burned areas in open shrublands, evergreen forest, needle-leaved and semi-deciduous forests is not known. In this study we tested the utility of Sentinel-2 derived spectral indices in burned area mapping. We sought to find out whether out of nine burned mapping indices, there exists a highly accurate spectral index to use in mapping burned areas in four distinct landcover types. The indices were selected based on their frequent use in burned area mapping.

Methods and Materials

Study area

Our hypothesis was tested in four randomly selected study sites located in different land cover types (Fig. 1). The study sites are located in different parts of the world and the landcover differs for each study site. The study sites were chosen based on their fire history which makes them suitable for use in wildfire studies. A brief description of the study sites is presented in Table 1.

Burned areas are influenced by several factors that include vegetation type, climatic variables and elevation [13]. In site 1 (Tenterfield, Australia), the area does not burn frequently but overall weekly bushfires were estimated to have increased by 40% in 2013 [15]. The land-use in site 1 includes patches of forest and farmlands. Site 2 (Pedrógão Grande, Portugal), is frequently burned and the wildfires are largely driven by climate and thermo-dynamical changes [47,52]. Study site 2 is in a human-dominated landscape. Study site 3 (California, United States of America) is in the western part of the USA and the area is characterised by frequent fires dating back to ~1500, before Euro-American settlement [33]. Some of these fires include the Santiago Fire of 1889 and the Laguna fire of 1970 [28]. Study site 3 (Hwange, Zimbabwe) is within a wildfire hotspot in Zimbabwe. The area frequently burns from poaching related fires [36].

Image Acquisition and Pre-processing

Cloud-free imagery from the Sentinel-2 sensor was downloaded from https://earthexplorer.usgs.gov/ (Accessed 10/10/2017). The images provided were already geometrically corrected but we further atmospherically corrected the images to derive the surface reflectance in QGIS using the Dark Object Subtraction (DOS-1) algorithm [51]. The algorithm corrects atmospheric effects (e.g. scattering) by subtracting each pixel with dark objects from pixels in the imagery, this is done for each respective band [6].

The mapping of burned areas within our study sites followed two processes that were (i) calculating spectral indices and (ii) using random classifiers to classify burned areas.

Table 1
The biophysical characteristics of the four study sites used in this study.

Study Site	Country	Location	Annual Temperature	Annual Precipitation	Landcover type	Date of Burn	Sentinel-2 Scene
Site 1	Australia	152° 4′ 4.728′′ E 29° 6′ 20.304′′ S	7.0°C - 26°C	52.7mm-109.8 mm	Semi-deciduous forest [3]	11/02/2017- 12/02/2017	L1C_T55HGE
Site 2	Portugal	7° 6′ 59.688′′ W 41° 45′ 28.08′′ N	8.5°C - 2.4°C	900mm- 1010 mm	Evergreen Forest [3]	17/06/2017- 24/06/2017	L1C_T29TNE
Site 3	USA	120° 21′ 35.244′′ W 40° 36′ 0′′ N	7.8°C- 14.6°C	800m- 1028 mm	Broad leaved deciduous forest [3]	27/07/2018- 18/09/2018	L1C_T29TNE
Site 4	Zimbabwe	28° 12′ 46.908′′ E 19° 17′ 33.612′′ S	17.5°C-33°C	500mm- 850 mm	Open Shrubland [3]	15/09/2017- 17/09/2017	L1C_T35KPU

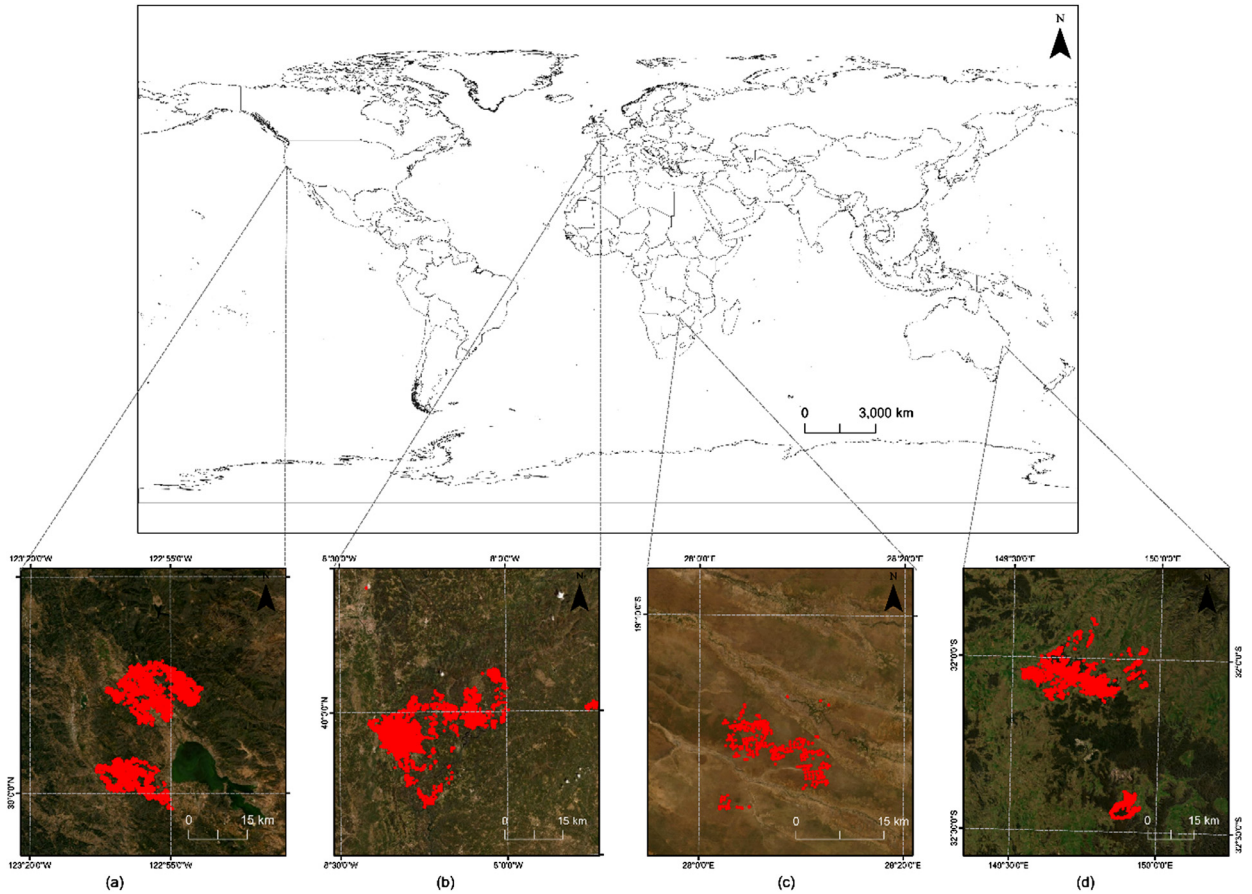

Fig. 1. Study sites that were used to test our hypothesis. The red dots represent data that were used to train and test the random forest algorithm.

Spectral indices

Nine post-fire burned mapping indices were calculated from the processed Sentinel-2 imagery. Although there exists vast literature on burned mapping indices, we selected the commonly used burned mapping indices to test our hypothesis [19,34]. All the indices that use the red band were optimized using the red-edge band. The optimization followed recommendations by Adelabu et al. [1] and Fernández-Manso et al. [19], who found out that the red-edge is sensitive to changes in chlorophyll. These changes in chlorophyll are common in burned areas [39] and the inclusion of the red-edge spectral band instead of the conventional red band could likely improve burned area detection. Information on the burned mapping indices used is provided in Table 2.

Classification

Image classification of the burned mapping indices was done using the random forest classifier in R [44] with the caret package [29]. Random forest uses classification and regression trees to build an ensemble model from averaging several other trees [4]. Important in implementing random forest is defining the number of variables that should be randomly selected at each tree node (m_{try}) as well as the number of trees (n_{trees}) that should be grown [31]. Increasing the number of trees allows the generalization error for each tree to eventually become constant**.** To determine the $m_{try\ and}$ n_{trees} to use that would optimize model performance we used tenfold cross-validation repeated thrice from a range of 1-6 m_{try} and 50-1500 n_{trees} This optimization process was done with the caret package [30]. Finally, nine random forest models were built and each model had one spectral index.

For image classification, burned areas were trained using Visible Infrared Imaging Radiometer Suite (VIIRS) active fire data downloaded from https://firms.modaps.eosdis.nasa.gov/ (accessed 10/10/2018). Unburned areas were trained using photo-interpreted Sentinel-2 MSI post-fire imagery following Ngadze et al. [39] and Mpakairi et al. [35]. The burned and unburned point data were split, and seventy percent were used for model training and thirty percent for model validation. Validation was performed using the overall accuracy measure. The measure has been widely used with machine learning algorithms to measure correctly classified objects using a validation dataset [10]. The overall accuracy ranges from 0 to 100. 0 representing

Table 2
Burned mapping indices used in the study area. The original red band used with these indices was replaced by the second red-edge band in Sentinel-2 MSI.

Name of Spectral Index	Formulae	Reference
Burned Area Index (BAI)	$\frac{1}{(0.1-Red_{edge})^2+(0.06-NIR)^2}$	[8]
Burned Area Index for Sentinel 2 (BAI2)	$1-\sqrt{(\frac{B6*B7*B8A}{B4})}*\frac{B12-B8A}{\sqrt{(B12+B8A)}}+1$ B4=Red; B6=Red_{edge}; B7= Red_{edge}; B8A=NIR; B12=SWIR	[20]
Char Soil Index (CSI)	$\frac{NIR}{SWIR}$	[50]
Enhanced Vegetation Index (EVI)	$\frac{2.5(NIR-Red_{edge})}{NIR+c_1 Red_{edge}-c_2 Blue+l}$ C_1=6.0; C_2=7.5; l=1	[23]
Global Environmental Monitoring Index (GEMI)	$\eta\ (1-0.25\eta)\ \frac{(Red_{edge}-0.125)}{1-Red\_edge}$ $\eta=\frac{2(Nir^2-Red_{edge}^2)+1.5*Nir+0.5*Red_{edge}}{Nir+Red_{edge}+0.5}$	[53]
Modified Soil-Adjusted Vegetation Index (MSAVI)	$\frac{2NIR+1-\sqrt{(2NIR+1)^2-8(NIR-Red_{edge})}}{2}$	[45]
Normalised Difference Vegetation Index (NDVI)	$\frac{(Nir-Red_{edge})}{(Nir-Red_{edge}}$	[37]
Normalized Burn Ratio (NBR)	$\frac{(Nir-SWIR)}{(Nir-SWIR}$	[18]
Optimized Soil Adjusted Vegetation Index (OSAVI)	$(1+L)\frac{Nir-Red_{edge}}{Nir+Red_{edge}+L}$ L=0.16	[26,45]

Table 3
Overall accuracy (OA) of classification using burn mapping indices with the random forest algorithm. OA ranges from 0 to 1. With high values indicating perfect agreement and low values indication disagreement.

Mapping index	Site Site 1 (Semi-deciduous forest)	Site 2 (Evergreen Forest)	Site 3 (Broad leaved deciduous forest)	Site 4 (Open Shrubland)
BAI_edge	0.93	0.92	0.88	0.90
BAI_2	0.92	0.90	0.87	0.83
CSI	0.91	0.90	0.86	0.78
EVI_edge	0.91	0.90	0.86	0.79
GEMI_edge	0.92	0.91	0.90	0.83
MSAVI_edge	0.92	0.91	0.86	0.80
NBR	0.91	0.90	0.86	0.76
NDVI_edge	0.91	0.91	0.86	0.70
OSAVI_edge	0.90	0.90	0.85	0.77

strong disagreement and 100 representing strong agreement. For each study site, the spectral index that had the highest accuracy was deemed the best index for burned area mapping for that respective study site.

Results

Our results show that BAI and GEMI outperformed the other seven burned area mapping indices in the four study sites (Table 3). On average, within the four study sites, BAI and GEMI had an overall accuracy that was $>$ 0.90. BAI performed best in semi-deciduous forests (site 1), evergreen forests (site 2) as well as open shrublands (site 4). Although GEMI had high accuracy in most study sites, it performed best in open needle-leaved deciduous forests (site 3).

The lowest-performing post-fire indices in the four study sites were OSAVI and NBR. OSAVI was the least performing in mapping fires in needle-leaved deciduous forests (site 1) and open needle-leaved deciduous forests (site 3). NBR was the least performing in mapping open shrublands and had an accuracy of 0.76. This was the lowest accuracy observed in all study sites. Noteworthy is the performance of the post-fire spectral bands in site 2. In evergreen forests (site 2), the difference between the best and least performing indices was 2% since all the indices had an overall accuracy $>$ 0.9.

Discussion

The difference in structure and composition of landcover types requires accurate mapping of burned areas by land managers and ecologists. In this study, out of nine burned mapping indices, we tested which index outperformed the others in different land cover types. Our results support as well as contradict previous literature about burned area mapping with spectral indices.

We found out that, of the nine post-fire burned area mapping indices that were tested in the four study sites, two indices (BAI and GEMI) outperformed the other indices. When optimized with the red-edge band BAI was able to map burned areas with high accuracy in open shrublands, evergreen and semi-deciduous forest. Open shrublands are typical of savannah ecosystems and require burned area spectral indices that can account for soil reflectance. Optimizing BAI with the red-edge band allowed it to account for soil reflectance as well as to detect the loss in vegetation through the near-infrared and red-edge band. BAI has been used broadly in fire mapping studies especially in Mediterranean ecosystems [7] where most

burning leaves behind with charcoal residuals. Our results are promising for the potential use of BAI in burned area mapping of savannah ecosystems, with high burn severity. This is supported by our observations since there was a difference of ~15% between BAI and the least performing index (NBR). However, Smith et al. [49] argued that using BAI in savannah ecosystems with low albedo surfaces (tilled soil) can overestimate burned areas. In another study using Landsat 8-OLI, Mpakairi et al. [35] observed that OSAVI performed better than most indices when used in savannah environments. Our results on the performance of optimised BAI in mapping fires in evergreen forests is new and outperforms the newly introduced BAI2 spectral index that uses the red-edge and short-wave domain, in discriminating burned and unburned areas [20]. However, the possibility of using BAI2 in mapping burned areas in evergreen forests is fairly new since its proposal by Filipponi [20].

GEMI performed well in mapping fires in broad-leaved forests as compared to the other red-edge optimized spectral indices that were tested. Broad-leaved forests usually allow dry matter to accumulate which is necessary for combustion [2,11]. The existence of dry matter can also result in high burn severity, which could have allowed GEMI to straightforwardly detect burned areas. GEMI has shown high accuracy in burned area mapping in areas with high burn severity (e.g. in Pereira [41] and Oliva et al. [40]). Additionally, in our study, the GEMI spectral index utilises the NIR and Red edge spectral regions for burned area mapping [16]. The NIR and Red are sensitive to burned areas since burned vegetation has a pronounced low reflection in the NIR region [42,43]. Spectral indices that utilize the Red edge and NIR spectral region are useful as they can detect burned areas regardless of the extent of vegetation damage. The high performance of GEMI in burned area mapping has been extensively tested and our findings are congruous to similar studies done by Burton et al. [5], Schepers et al. [48] and Epting and Verbyla [17].

Before the introduction of spectral indices in burned area mapping, estimating the area burned after a wildfire was an enormous task for most ecologists. Although several spectral indices for burn mapping have been proposed, most of these indices work best in certain environments owing to the variability in burn severity, vegetation structure and composition in most environments [7,12,21]. Besides, most of these spectral indices require multi-temporal analysis (i.e. pre and post-fire images). However, what remains critically important is for a spectral index used with a sensor that can spatially and spectrally discriminate between a burned and an unburned pixel.

Although Sentinel-2 (10m) is a medium resolution sensor, it has allowed for improved mapping of fires at a finer spatial and spectral scale as compared to other sensors. Previous sensors that were available had courser resolutions, for instance, AVHRR (1km), MODIS (250m) and Landsat (30m). Accounting for spatial variability in pixels that are not fully burned is computationally intensive when using coarse resolution imagery. Hence, the improved spatial resolution of Sentinel-2 allows for high accuracy in discriminating burned and unburned pixels for small fires [14]. Consequently, our study presents how post-fire burned mapping is possible with Sentinel-2 given the finer resolution as compared to other medium-resolution sensors [25]. Although there exists vast literature on how vegetation is sensitive in the red-edge band and how the red-edge band can enhance the performance of most spectral indices, most studies on burned mapping have used the original versions of the spectral indices instead (e.g. Fraser et al. [21], Smith et al. [49] and Smith et al. [50]). Hence, results from this study are consenting since we took advantage of the red-edge band available from Sentinel-2 and used it to optimize the already present spectral indices for improved burned area discrimination.

Conclusion

Although numerous spectral indices for burned area mapping are available, selecting the best spectral indices for a particular study site could be difficult especially when it has been used in several study sites. In this study, we aimed to find out whether out of the nine burned mapping spectral indices, there was an index that outperformed other indices in the four land cover types. We found out that Burned Area Index (BAI) and Global Monitoring Environment Index (GEMI) outperform other indices in open shrublands, evergreen forest and needle-leaved and semi-deciduous forests. These results could provide necessary insight for burned mapping algorithms and accurate estimation of post-fire carbon emission in open shrublands, evergreen, needle-leaved and semi-deciduous forests.

Declaration of Competing Interest

The authors declare that they have no known competing financial interests or personal relationships that could have appeared to influence the work reported in this paper.

CRediT authorship contribution statement

Kudzai Shaun Mpakairi: Conceptualization, Methodology, Writing - original draft. **Henry Ndaimani:** Conceptualization, Writing - review & editing. **Blessing Kavhu:** Writing - review & editing.

Reference

[1] S. Adelabu, O. Mutanga, E. Adam, Evaluating the impact of red-edge band from Rapideye image for classifying insect defoliation levels, ISPRS Journal of Photogrammetry and Remote Sensing 95 (2014) 34–41.
[2] B. Berg, H. Staaf, Leaching, accumulation and release of nitrogen in decomposing forest litter, Ecol. Bull 33 (1981) 163–178.
[3] Bontemps, S., P. Defourny, E. V. Bogaert, O. Arino, V. Kalogirou, and J. R. Perez. 2011. GLOBCOVER 2009-Products description and validation report.

[4] L. Breiman, Random forests, Machine learning 45 (2001) 5–32.
[5] P.J. Burton, M.-A. Parisien, J.A. Hicke, R.J. Hall, J.T. Freeburn, Large fires as agents of ecological diversity in the North American boreal forest, International Journal of Wildland Fire 17 (2009) 754–767.
[6] P.S. Chavez Jr, An improved dark-object subtraction technique for atmospheric scattering correction of multispectral data, Remote Sensing of Environment 24 (1988) 459–479.
[7] E. Chuvieco, M.P. Martin, A. Palacios, Assessment of different spectral indices in the red-near-infrared spectral domain for burned land discrimination, International Journal of Remote Sensing 23 (2002) 5103–5110.
[8] E. Chuvieco, M.P. Martín, A. Palacios, Assessment of different spectral indices in the red-near-infrared spectral domain for burned land discrimination, International Journal of Remote Sensing 23 (2002) 5103–5110.
[9] J.G. Clevers, A.A. Gitelson, Remote estimation of crop and grass chlorophyll and nitrogen content using red-edge bands on Sentinel-2 and-3, International Journal of Applied Earth Observation and Geoinformation 23 (2013) 344–351.
[10] R.G. Congalton, A review of assessing the accuracy of classifications of remotely sensed data, Remote sensing of environment 37 (1991) 35–46.
[11] E. Cuevas, S. Brown, A.E. Lugo, Above-and belowground organic matter storage and production in a tropical pine plantation and a paired broadleaf secondary forest, Plant and soil 135 (1991) 257–268.
[12] J. Delegido, J. Verrelst, C. Meza, J. Rivera, L. Alonso, J. Moreno, A red-edge spectral index for remote sensing estimation of green LAI over agroecosystems, European Journal of Agronomy 46 (2013) 42–52.
[13] S.H. Doerr, C. Santín, Global trends in wildfire and its impacts: perceptions versus realities in a changing world, Philosophical transactions of the Royal Society of London. Series B, Biological sciences 371 (2016) 20150345.
[14] M. Drusch, U. Del Bello, S. Carlier, O. Colin, V. Fernandez, F. Gascon, B. Hoersch, C. Isola, P. Laberinti, P. Martimort, Sentinel-2: ESA's optical high-resolution mission for GMES operational services, Remote sensing of environment 120 (2012) 25–36.
[15] R. Dutta, A. Das, J. Aryal, Big data integration shows Australian bush-fire frequency is increasing significantly, Royal Society open science 3 (2016) 150241.
[16] J. Eidenshink, B. Schwind, K. Brewer, Z.-L. Zhu, B. Quayle, S. Howard, A project for monitoring trends in burn severity, Fire ecology 3 (2007) 3–21.
[17] J. Epting, D. Verbyla, Landscape-level interactions of prefire vegetation, burn severity, and postfire vegetation over a 16-year period in interior Alaska, Canadian Journal of Forest Research 35 (2005) 1367–1377.
[18] S. Escuin, R. Navarro, P. Fernandez, Fire severity assessment by using NBR (Normalized Burn Ratio) and NDVI (Normalized Difference Vegetation Index) derived from LANDSAT TM/ETM images, International Journal of Remote Sensing 29 (2008) 1053–1073.
[19] A. Fernández-Manso, O. Fernández-Manso, C. Quintano, SENTINEL-2A red-edge spectral indices suitability for discriminating burn severity, International Journal of Applied Earth Observation and Geoinformation 50 (2016) 170–175.
[20] Filipponi, F. 2018. BAIS2: Burned Area Index for Sentinel-2. Page 364 in Multidisciplinary Digital Publishing Institute Proceedings.
[21] R. Fraser, Z. Li, J. Cihlar, Hotspot and NDVI differencing synergy (HANDS): A new technique for burned area mapping over boreal forest, Remote Sensing of Environment 74 (2000) 362–376.
[22] L. Giglio, J.T. Randerson, G.R. van der Werf, Analysis of daily, monthly, and annual burned area using the fourth-generation global fire emissions database (GFED4), Journal of Geophysical Research: Biogeosciences 118 (2013) 317–328.
[23] A. Heute, H. Liu, K. Batchily, W. Van Leeuwen, A comparison of vegetation indices over a global set of TM images for EOS-MODIS, REMOTE SENSING OF ENVIRONMENT-NEW YORK- 59 (1997) 440–451.
[24] J.J. Hoelzemann, M.G. Schultz, G.P. Brasseur, C. Granier, M. Simon, Global Wildland Fire Emission Model (GWEM): Evaluating the use of global area burnt satellite data, Journal of Geophysical Research: Atmospheres 109 (2004).
[25] M. Immitzer, F. Vuolo, C. Atzberger, First experience with Sentinel-2 data for crop and tree species classifications in central Europe, Remote Sensing 8 (2016) 166.
[26] Karimi, A., S. Abdollahi, K. Ostad-Ali-Askari, S. Eslamian, and V. P. Singh. 2018. Predicting Fire Hazard Areas Using Vegetation Indexes, Case Study: Forests of Golestan Province, Iran. Journal of Geography and Cartography.
[27] R.E. Keane, R. Burgan, J. van Wagtendonk, Mapping wildland fuels for fire management across multiple scales: integrating remote sensing, GIS, and biophysical modeling, International Journal of Wildland Fire 10 (2001) 301–319.
[28] J.E. Keeley, P.H. Zedler, Large, high-intensity fire events in southern California shrublands: debunking the fine-grain age patch model, Ecological Applications 19 (2009) 69–94.
[29] M. Kuhn, The caret package, R Foundation for Statistical Computing, Vienna, Austria, 2012 URL https://cran.r-project.org/package=caret .
[30] M. Kuhn, J. Wing, S. Weston, A. Williams, C. Keefer, A. Engelhardt, T. Cooper, Z. Mayer, B. Kenkel, caret: Classification and regression training, R package version 6 (2015) 0–21 CRAN, Vienna, Austria.
[31] A. Liaw, M. Wiener, Classification and regression by randomForest, R news 2 (2002) 18–22.
[32] T.V. Loboda, E.E. Hoy, L. Giglio, E.S. Kasischke, Mapping burned area in Alaska using MODIS data: a data limitations-driven modification to the regional burned area algorithm, International Journal of Wildland Fire 20 (2011) 487–496.
[33] C. Mallek, H. Safford, J. Viers, J. Miller, Modern departures in fire severity and area vary by forest type, Sierra Nevada and southern Cascades, California, USA, Ecosphere 4 (2013) art153.
[34] J.D. Miller, A.E. Thode, Quantifying burn severity in a heterogeneous landscape with a relative version of the delta Normalized Burn Ratio (dNBR), Remote Sensing of Environment 109 (2007) 66–80.
[35] K.S. Mpakairi, S.L. Kadzunge, H. Ndaimani, Testing the utility of the blue spectral region in burned area mapping: Insights from savanna wildfires, Remote Sensing Applications: Society and Environment 20 (2020) 100365.
[36] K.S. Mpakairi, P. Tagwireyi, H. Ndaimani, H.T. Madiri, Distribution of wildland fires and possible hotspots for the Zimbabwean component of Kavango-Zambezi Transfrontier Conservation Area, South African Geographical Journal (2018) 1–11.
[37] O. Mutanga, E. Adam, M.A. Cho, High density biomass estimation for wetland vegetation using WorldView-2 imagery and random forest regression algorithm, International Journal of Applied Earth Observation and Geoinformation 18 (2012) 399–406.
[38] Nature, The complexities of wildfires, Nature Geoscience 12 (2019) 81.
[39] F. Ngadze, K.S. Mpakairi, B. Kavhu, H. Ndaimani, M.S. Maremba, Exploring the utility of Sentinel-2 MSI and Landsat 8 OLI in burned area mapping, for a heterogenous savannah landscape, PLoS ONE 15 (2020) e0232962.
[40] P. Oliva, P. Martín, E. Chuvieco, Burned area mapping with MERIS post-fire image, International journal of remote sensing 32 (2011) 4175–4201.
[41] J.M. Pereira, A comparative evaluation of NOAA/AVHRR vegetation indexes for burned surface detection and mapping, IEEE Transactions on Geoscience and Remote sensing 37 (1999) 217–226.
[42] J.M. Pereira, A.C. Sá, A.M. Sousa, J.M. Silva, T.N. Santos, J.M. Carreiras, Spectral characterisation and discrimination of burnt areas, Pages 123-138 Remote sensing of large wildfires, Springer, 1999.
[43] M. Pleniou, N. Koutsias, Sensitivity of spectral reflectance values to different burn and vegetation ratios: A multi-scale approach applied in a fire affected area, ISPRS Journal of Photogrammetry and Remote Sensing 79 (2013) 199–210.
[44] R Core, T. 2013. R: A language and Environment for Statistical Computing. Vienna, Austria.
[45] J. Rogan, S. Yool, Mapping fire-induced vegetation depletion in the Peloncillo Mountains, Arizona and New Mexico, International Journal of Remote Sensing 22 (2001) 3101–3121.
[46] J. San-Miguel-Ayanz, J.M. Moreno, A. Camia, Analysis of large fires in European Mediterranean landscapes: lessons learned and perspectives, Forest Ecology and Management 294 (2013) 11–22.
[47] A. Sánchez-Benítez, R. García-Herrera, D. Barriopedro, P.M. Sousa, R.M. Trigo, June 2017: the earliest European summer mega-heatwave of Reanalysis Period, Geophysical Research Letters 45 (2018) 1955–1962.

[48] L. Schepers, B. Haest, S. Veraverbeke, T. Spanhove, J. Borre, V, R. Goossens, Burned Area Detection and Burn Severity Assessment of a Heathland Fire in Belgium Using Airborne Imaging Spectroscopy (APEX), Remote Sensing 6 (2014) 1803–1826.
[49] A. Smith, N. Drake, M. Wooster, A. Hudak, Z. Holden, C. Gibbons, Production of Landsat ETM+ reference imagery of burned areas within Southern African savannahs: comparison of methods and application to MODIS, International Journal of Remote Sensing 28 (2007) 2753–2775.
[50] A.M. Smith, M.J. Wooster, N.A. Drake, F.M. Dipotso, M.J. Falkowski, A.T. Hudak, Testing the potential of multi-spectral remote sensing for retrospectively estimating fire severity in African Savannahs, Remote Sensing of Environment 97 (2005) 92–115.
[51] Team, Q. D. 2015 a. QGIS geographic information system. Open Source Geospatial Foundation Project. Disponível em:< http://www.qgis.org/). Acesso em 27.
[52] M. Turco, S. Jerez, S. Augusto, P. Tarín-Carrasco, N. Ratola, P. Jiménez-Guerrero, R.M. Trigo, Climate drivers of the 2017 devastating fires in Portugal, Scientific Reports 9 (2019) 13886.
[53] C. Wright, A. Gallant, Improved wetland remote sensing in Yellowstone National Park using classification trees to combine TM imagery and ancillary environmental data, Remote Sensing of Environment 107 (2007) 582–605.